Republic of Iraq
Ministry of Higher
Education
and Scientific Research
University of Diyala
College of Science
Department of Physics

Synthesis and Characterization of Inorganic – Polyaniline Hybrid Nanostructures for Sensing Applications

A thesis
Submitted to the Council of the College of Science
University of Diyala in Partial Fulfillment of Requirements for
the Degree of Doctor of Philosophy in Physics
By

Ahmed Mohammed Shano

B.Sc. 2012

M.Sc. 2015

Supervised By

Prof. Dr.
Nabeel A. Bakr

2018 A.D.

Prof. Dr.
Iftikhar M. Ali

1440 A.H.

بِسْمِ اللهِ الرَّحْمنِ الرَّحِيمِ

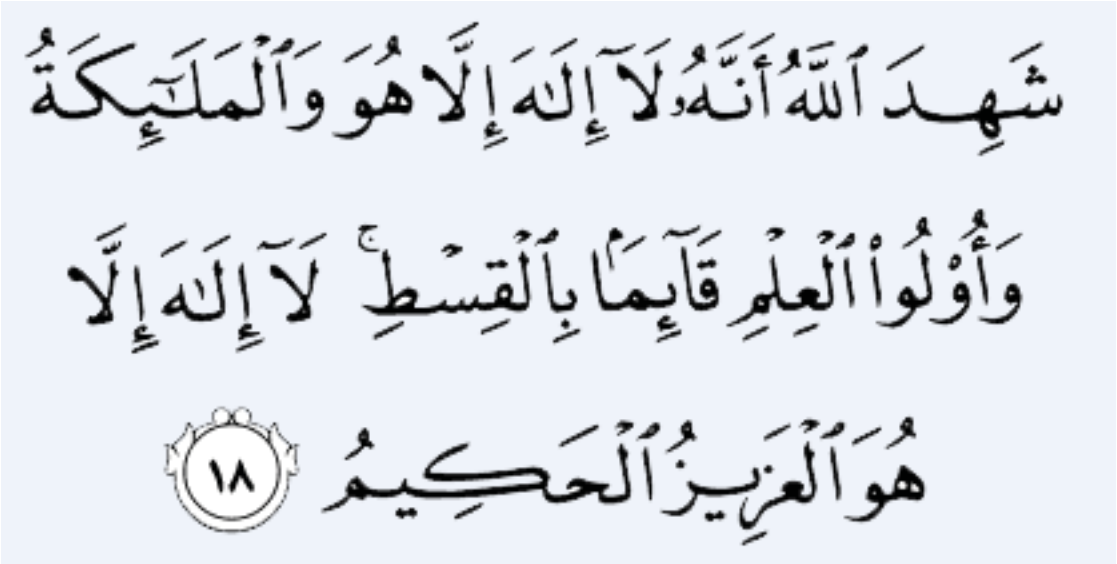

صدق الله العظيم

سورة آل عمران: الآية ١٨

Dedication

To …….

The lights of my life

Father & Mother

The lights of my eyes

Brothers, Sisters and My Friends

All faithful hearts who helped me
in the journey of my life.

Ahmed

Acknowledgement

First of all I thank the Almighty ***Allah***, whose Grace enabled me to continue this work and overcome all difficulties and our prophet ***Muhammad*** (peace and blessings of Allah be upon him) who invites us to science and knowledge.

I would like to express my sincere appreciation and deep gratitude to my supervisors, **Prof. Dr. Nabeel A. Bakr** and **Prof. Dr. Iftikhar M. Ali** for suggesting the topic of this thesis, guidance, suggestions and continuous encouragement throughout the research work

I would like to express my profound gratitude to **Prof. Dr. Sabah A. Salman** for his kind cooperation and constant support. I am highly indebted to **Assist. Prof Dr. Ziad T. Khodair** for his constant encouragement throughout my Ph.D. study in the Department of Physics, College of Science, University of Diyala.

Special thanks are extended to the University of Diyala, College of Science, specially The dean of College of Science, **Prof. Dr. Tahseen H. Mubarak** and the head of the department, **Dr. Jasim M. Mansoor** and all the Staff of the Department of Physics for their assistance.

I would also like to thank the staff of the Library of College of Science(**Adnan and Raafat**), who continued to provide excellent service, tireless support and scientific resources to all students.

I do not forget to thank **Assist. Prof. Dr. Issam M. Ibrahim** (Baghdad University), and Physics Department staff for their support.

I am grateful to the staff of thin film laboratory and my colleagues at Physics Dept. College of Science, University of Baghdad, **Marwan, Abeer, Suhaad and Masar.**

My greatest indebtedness goes to my **Father, Mother and Brothers** for their valuable advice, and to my Friends (**Aws, Wisam, Ali, Adnan, Abo Ayman, Mohammed Alazawi, Waleed, Ibrahim, Haidar, Marwan, Bashar, Kadhim Al-Jumaily, Anwar and Sufian)** for their endless support.

Supervisor Certification

We certify that this thesis entitled **"Synthesis and Characterization of Inorganic – Polyaniline Hybrid Nanostructures for Sensing Applications"** for the student (**Ahmed Mohammed Shano**), was prepared under our supervisions at the Department of Physics, College of Science, University of Diyala in partial fulfillment of requirements needed to award the degree of **Doctor of Philosophy (Ph.D.) in Physics.**

Signature: N. A. Bakr

Name: **Dr. Nabeel A. Bakr**

Scientific Degree: Professor

Address: College of Science,

University of Diyala

Date: 25 / 9 / 2018

Signature:

Name: **Dr. Iftikhar M. Ali**

Scientific Degree: Professor

Address College of Science

University of Baghdad

Date: 25 / 9 / 2018

In view of the available recommendations, we forward this thesis for debate by the examination committee.

Signature:

Name: **Dr. Jasim M. Mansoor**

Scientific Degree: Lecturer

Head of the Physics Department

Address: College of Science, University of Diyala

Date: 30 / 9 / 2018

Linguistic Amendment

I certify that the thesis entitled "**Synthesis and Characterization of Inorganic – Polyaniline Hybrid Nanostructures for Sensing Applications**" presented by (**Ahmed Mohammed Shano**), has been corrected linguistically, therefore, it is suitable for debate be examining committee.

Signature:

Name: **Nizar. H. Wali**

Scientific Degree: Assistant Professor

Address: English Department, College of Basic Education, University of Diyala

Date: 23 / 9 / 2018

Scientific Amendment

I certify that the thesis entitled (**Synthesis and Characterization of Inorganic – Polyaniline Hybrid Nanostructures for Sensing Applications**) presented by (**Ahmed Mohammed Shano**), has been evaluated scientifically, therefore, it is suitable for debate be examining committee.

Signature:

Name: **Dr. Estabraq T. Abdullah**

Scientific Degree: Assistant Professor

Address: Physics Department/ College of Science/ University of Baghdad

Date: 24 / 9 / 2018

Examination Committee Certificate

We certify that we have read this thesis entitled " **Synthesis and Characterization of Inorganic – Polyaniline Hybrid Nanostructures for Sensing Applications** " and, as an examining committee, we examined the student (**Ahmed Mohammed Shano**) on its content and in what is related to it, and that in our opinion it meets the standard of a thesis for the degree of Doctor of Philosophy in Physics.

Signature
Name: **Prof. Dr. Nadir F.Habubi**
Address: Al-Mustansiriyah University
Data: 25 / 9 / 2018
Chairman

Signature
Name: **Prof Dr. Ibrahim. R. Agool**
Address: Bilad Alrafidain University College
Data: 24 / 9 / 2018
Member

Signature
Name: **Prof. Dr. Sabah A. Salman**
Address: University of Diyala
Data: 25 / 9 / 2018
Member

Signature
Name: **Assist. Prof. Dr. Abdulhadi K. Jedran**
Address: University of Technology
Data: 25 / 9 / 2018
Member

Signature
Name: **Assist. Prof. Dr. Ziad T. Khodair**
Address: University of Diyala
Data: 23 / 9 / 2018
Member

Signature
Name: **Prof. Dr. Nabeel A. Bakr**
Address: University of Diyala
Data: 25 / 9 / 2018
Supervisor

Signature
Name: **Prof. Dr. Iftikhar M. Ali**
Address: University of Baghdad
Data: 25 / 9 / 2018
Supervisor

Approved by the Council of the College of Science.
(The Dean)
Signature:
Name: **Prof. Dr. Tahseen H. Mubarak**
Date: 30 / 9 / 2018

Published and Accepted Research Articles

1. Iftikhar M. Ali, Ahmed M. Shano and Nabeel A. Bakr, "H_2S gas sensitivity of PAni nano fibers synthesized by hydrothermal method", Journal of Materials Science: Materials in Electronics, Springer, Vol. 29, pp.11208–11214(2018)

2. Ahmed M. Shano, Iftikhar M. Ali and Nabeel A. Bakr," Photo-detecting properties of polyaniline/CuO nanostructures synthesized by hydrothermal technique", Science International in Service Since 1988, (communicated)

Abstract

In this study, PAni NFs and metal oxides nanostructures [tin oxide (SnO_2) and copper oxide (CuO)] have successfully synthesized by using hydrothermal method and depositing PAni NFs, SnO_2 and CuO and their composites on silicon and glass substrates by spin coating technique at room temperature with thickness of about 325 nm. The structural, surface morphological, optical, electrical, photoconductivity and gas sensing properties have been investigated for Inorganic – Polyaniline films. The XRD results showed that PAni films have crystalline nature, SnO_2 and PAni/SnO_2 nanostructure composite are polycrystalline in nature with tetragonal structure , CuO and PAni/CuO nanostructure composite are polycrystalline in nature with Monoclinic structure, The crystallite size is estimated by Scherrer formula and W-H analyses and it is found that it increases as the concentration ratio of SnO_2 and CuO increasing. The FESEM images of Polyaniline clearly indicate that the polymer possesses nanofiber like structure, where's the SnO_2 and CuO films have cauliflower like and regular shapes respectively. The surface morphology of composites are nanofiber caped with inorganic material which are SnO_2 and CuO as core-shell structure. The optical properties show that the energy gap follows allowed direct electronic transition calculated using Tauc's equation and it is noticed that the band gap value decreases as the SnO_2, CuO ratios increases. PL showed that peaks intensity increases as the concentration of SnO_2 and CuO increases. The electrical properties include Resistance–Temperature Characteristic, D.C. electric conductivity and Hall effect measurements. The resistance of the films decreases as the temperature increased which shows a semiconductor behavior and activation energies and electrical conductivity (σ_{RT}) are decreases with increasing

of addition of inorganic semiconductors into PAni NFs. The results of Hall coefficient showed p-type semiconductor behavior for all films except that for pure SnO_2 films which is n-type. The built-in potential (V_{bi}) increases with increasing by addition of inorganic composites into polymer matrix. The photoconductivity properties, in current-voltage (I-V) characteristics, the value of ideality factor and tunneling factor increase with increasing by adding of inorganic semiconductors into polymer matrix, the responsivity, G%, D and D* increase with increases of SnO_2 and CuO nanostructures ratio except NEP is decreases, and the current -time (I-t) characteristics investigate that the response had square pulse for UV-Vis light region that means fast response for all films. The sensitivity to H_2S gas increased with increases of operating temperatures and SnO_2 and CuO concentration. The maximum sensitivity to H_2S gas was observed to nanocomposites PAni/CuO films at high amount of CuO and found to be 260 % at (T_o= 200 ^oC). The response and recovery time increased with increase in operating temperature and SnO_2 and CuO concentration and the nanocomposites PAni/CuO films at concentration 3mL from CuO exhibits a fast response speed (0.753s) with recovery time (0.787s) at (30^oC), while the slow response speed was observed for 7mL CuO (0.921s) with recovery time of (0.857s).

List of Contents

No.	Subjects	Page No.
Chapter One Introduction and Basic Concept		
1.1	Introduction	1
1.2	The Physics of Nano Dimensional Material	2
1.3	Conducting Polymers	2
1.4	Conjugated Polymer	3
1.5	Polyaniline (PAni)	4
1.5.1	Different Oxidation States of PAni	6
1.5.2	Polyaniline Conductivity	7
1.6	Applications of Conducting Polymers	9
1.7	Hybrids of Conducting Polymers	10
1.7.1	Introduction of Hybrids	10
1.7.2	Classification of Hybrid Materials	11
1.7.3	Factors Influencing Properties of Hybrid Materials	12
1.7.4	Synthesis of Hybrid Materials	12
1.7.5	Applications of Hybrid Materials	14
1.8	Tin Oxides	15
1.9	Copper Oxide	16
1.10	Thin Films	18
1.11	Thin Films Deposition Techniques	19
1.11.1	Spin Coating Technique	19

1.12	Previous Studies	20
1.13	Objectives of The Study	29
Chapter Two Theoretical Background		
2.1	Introduction	30
2.2	X-Ray	30
2.3	Structure of Thin Films	30
2.4	Structural Parameters	30
2.4.1	Lattice Constant (a, c) of Tetragonal Structure	30
2.4.2	Lattice Constant (a, b, c) of Monoclinic Structure	31
2.4.3	Average Crystallite Size (D_{av})	31
2.4.4	Dislocation Density and Number of Grains	32
2.5	Fourier Transform Infrared Instruments (FTIR)	32
2.6	Optical Properties	33
2.7	Electronic Transitions	33
2.7.1	The Direct Transitions	33
2.7.2	The Indirect Transitions	35
2.8	Optical Constants	36
2.9	Optical Properties of Amorphous Semiconductors	37
2.9.1	High Absorption Region	37
2.9.2	Exponential Region	37
2.9.3	Low Absorption Region	38
2.10	Optical Energy Gap (Eg)	38
2.11	Photoluminescence (PL)	39

2.12	Electrical Properties	40
2.12.1	D.C. Conductivity	40
2.12.2	The Hall Effect	42
2.12.3	Capacitance –Voltage Characteristics	43
2.13	Photoconductivity (PC)	44
2.13.1	Current-Voltage Characteristics (I-V Plot)	45
2.13.2	Rise and Fall Times upon a Square-Pulse Signal	47
2.13.3	Spectral Response Measurements	47
2.13.4	Important Properties of Photodetectors	49
2.14	Gas Sensors	50
2.15	Gas Sensor Applications	51
2.16	Sensing Materials	52
2.17	Mechanism of Sensing	53
2.18	Interactions Between Gas Molecules and Conducting Polymer Films	54
2.19	Physical and Chemical Properties of H_2S Gas	55
2.20	Band Theory Applied to Sensors	56
2.21	Characteristics of Gas Sensors	56
2.21.1	Sensitivity	57
2.21.2	Response and Recovery Times	57
Chapter Three Experimental Work		
3.1	Introduction	58
3.2	Chemicals and Raw Materials	58
3.3	Substrates Preparation	66

3.3.1	Substrate Cleaning	60
3.4	Synthesis of Inorganic – Polyaniline nanostructures	61
3.4.1	Hydrothermal Method	61
3.4.2	Synthesis Polyaniline	62
3.4.3	Synthesis Metal Oxides {Tin Oxide (SnO_2) and Copper Oxide (CuO)}	63
3.4.4	Preparation Solutions Inorganic – Polyaniline Hybrid	64
3.5	Thin Film Preparation	64
3.5.1	Spin Coating Technique	64
3.6	Characterizations Techniques	66
3.6.1	Structural Measurements	66
3.6.2	Field Emission Scanning Electron Microscope (FESEM)	66
3.6.3	Fourier Transform Infrared (FTIR)Spectroscopy	66
3.6.4	Optical Measurements	67
3.6.5	Photoluminescence Measurement (PL)	68
3.6.6	Electrical Measurements	68
3.7	Photoconductivity	71
3.7.1	The photoconductivity Set up	71
3.7.2	Current - Voltage Measurements (I-V)	71
3.7.3	Spectral Response Measurements	72
3.8	Gas Sensor System	72
3.9	Gas Sensor Testing Set up	72
Chapter Four Results and discussion		
4.1	Introduction	75

4.2	Structural Properties of Inorganic – Polyaniline	75
4.2.1	XRD Analysis for PAni NFs, SnO_2 , CuO and nanostructure Composites of PAni/SnO_2 and PAni/CuO	75
4.2.2	The crystallite size (D_{av})	81
4.2.3	Dislocation Density (δ)	83
4.2.4	The Number of crystals (No)	83
4.3	Morphology Analysis	84
4.3.1	FESEM Analysis for PAni NFs, SnO_2 , CuO and nanostructure Composites of PAni/SnO_2 and PAni/CuO	84
4.4	Fourier transform infrared (FTIR) spectroscopic analysis	88
4.4.1	FTIR Analysis for Inorganic – Polyaniline	89
4. 5	Optical Properties	92
4.5.1	Absorbance (A)	93
4.5.2	Optical Energy Gap (E_g)	94
4.6	Photoluminescence (PL)	97
4.7	Electrical Properties	101
4.7.1	Resistance – Temperature Characteristic	101
4.7.2	D.C Conductivity	102
4.7.3	Hall Effect	105
4.7.3	C-V Characteristics	107
4.8	The Photoconductivity Measurements	111
4.8.1	I-V Characteristics	111
4.8.1.a	I-V Characteristics for PAni NFs in Dark	116
4.8.2	Characteristic of PAni NFs Photoconductor Device	118
4.9	Gas Sensing Result	128

4.9.1	Measurement of H_2S Gas	129
4.10	Conclusions	137
4.11	Future Work	138
	References	139

List of Tables

No.	Title	Page No.
1.1	The properties of SnO_2	16
1.2	The properties of CuO	18
2.1	Typical Sensing Materials Used in Gas Sensors	53
2.2	Semiconductor resistance change (increase or decrease) to change in gas atmosphere	56
3.1	Physical and chemical properties of the materials to synthesis polyaniline nano fibers	58
3.2	Physical and chemical properties of the materials used to synthesis metal oxides (SnO_2 and CuO)	60
4.1	X-ray diffraction results of PAni, SnO_2, CuO and their composites thin films.	80
4.2	Structural parameters for PAni and comparison between Scherrer and W-H methods of SnO_2, CuO and their composites with PAni thin films	84
4.3	Energy gap for PAni NFs, SnO_2 and CuO and their nanocomposite with different SnO_2 and CuO contents	97
4.4	D.C activation energies and electrical conductivity (σ_{RT}) for PAni NFs , SnO_2 and CuO and their nanocomposite with different SnO_2 and CuO contents	105
4.5	Hall parameters of PAni NFs, SnO_2 and CuO and their nanocomposite with different SnO_2 and CuO contents	106
4.6	Built in potential (V_{bi}) of PAni NFs, SnO_2 and CuO and their nanocomposite with different SnO_2 and CuO concentrations.	110
4.7	I_o, Φ_B, $\mathbf{A_t}$ and **n** values of PAni NFs, SnO_2 and CuO and their nanocomposite with different SnO_2 and CuO concentrations at	118

	dark	
4.8	The rise, fall times and sensitivity as a function of wavelength and mixing doping for PAni NFs, SnO_2 and CuO and their nanocomposite with different SnO_2 and CuO contents	121
4.9	Result of PC detector for PAni NFs, SnO_2 and CuO and their nanocomposite with different SnO_2 and CuO contents films at 250 nm illumination	128
4.10	Response time, recovery time and sensitivity % of PAni NFs, SnO_2 and CuO and their nanocomposite with different SnO_2 and CuO contents at different operating temperatures	136

List of Figures

No.	Title	Page No.
1.1	Intrinsically conducting polymers	3
1.2	Structure of the polyaniline chain	4
1.3	Different oxidation states of PAni, leuoemeraldine (LE), emeraldine base (EB), emeraldine salt (ES) and perningraniline (PN)	5
1.4	Different forms of polyaniline	7
1.5	Schematic presentation of conductivity for polyaniline	9
1.6	Classification of materials at different scale levels	11
1.7	Composites and hybrids with phases	12
1.8	The lattice structure of SnO_2	15
1.9	The lattice structure of CuO	17
1.10	Classification of thin film deposition techniques	20
2.1	Types of electronic transitions	30
2.2	The fundamental absorption edge and absorption Regions	38
2.3	Photoluminescence schematic	39
2.4	Geometry of the Hall Effect	43
2.5	Mechanism of photoconductivity	44

2.6	Current-voltage characteristics graph that shows schottky behavior	46
2.7	Rise and fall times for square-pulse signal	47
2.8	Schematic diagram of band bending after chemisorptions of charged species. Λ air: thickness of the space-charge layer, eV surface: potential barrier	54
3.1	Schematic diagram of experimental work	59
3.2	The hydrothermal reactor used in our study	62
3.3	Schematic illustration of the spin coating technique	65
3.4	An illustration of the process of nucleation (1), crystal growth (2) and film formation (3).	65
3.5	Block diagram for FTIR Spectrometer	67
3.6	Diagram showing how the UV–Visible spectrometer works	68
3.7	The circuit used for measuring D.C. conductivity	68
3.8	Mask for D.C. conductivity	69
3.9	A schematic illustration of the photoconductive device structure	70
3.10	Block diagram setup for measuring photoconductivity	71
3.11	Gas Sensing Measurement System	73
3.12	Schematic diagram of gas sensing and the electrical circuit setup	74
4.1	XRD pattern of PAni thin films	76
4.2	XRD patterns of SnO_2 thin films	77
4.3	XRD patterns of PAni/SnO_2 composites thin films	77
4.4	XRD pattern of CuO thin films	79
4.5	XRD patterns of PAni/CuO composites thin films	79
4.6	The W-H analysis of SnO_2 and CuO and their composite thin films with PAni (PAni/SnO_2 and PAni/CuO).	82
4.7	SEM images of PAni NFs (a) at low magnification (10 kx), (b) at high magnification (23kx).	85
4.8	FESEM images of SnO_2 nanostructures films at (a) 100 kx and (b) 200 kx magnifications	86
4.9	FESEM images of PAni/SnO_2 nanocomposite thin film for higher SnO_2 content(7mL) at (a) 100 kx and (b) 200 kx magnifications	86
4.10	FESEM images of CuO nanostructures films at (a) 100 kx and (b) 200 kx magnifications.	87

4.11	FESEM images of PAni/CuO nanocomposite thin films for higher CuO content(7mL) at (a) 100 kx and (b) 200 kx magnifications	88
4.12	The cross-sectional FESEM image for PAni/ SnO_2 nanocomposite thin film grown on Si wafer	88
4.13	FTIR transmittance spectra of PAni NFs	89
4.14	FTIR transmittance spectra of SnO_2 nanostructures and PAni/SnO_2 nanocomposite with different SnO_2 contents	91
4.15	FTIR transmittance spectra of CuO and PAni/CuO nanocomposite with different CuO contents	92
4.16	Absorbance spectra of PAni NFs, SnO_2 and CuO.	93
4.17	Absorbance spectra of PAni/SnO_2 nanocomposite with different SnO_2 contents.	94
4.18	Absorbance spectra of PAni/CuO nanocomposite nano composite with different CuO contents	94
4.19	Tauc's plot of PAni NFs	96
4.20	Tauc's plot of SnO_2 and its composites with PAni NFs	96
4.21	Tauc's plot of CuO and its composites with PAni NFs	97
4.22	Photoluminescence spectrum of (a) PAni NFs, (b) SnO_2 and (c) CuO	98
4.23	Photoluminescence spectra of PAni/SnO_2 nanocomposites	100
4.24	Photoluminescence spectra of PAni/CuO nanocomposites	100
4.25	The variation of resistance as a function of temperature for (a) PAni NFs, SnO_2 and CuO	101
4.26	The variation of resistance as a function of temperature of PAni/SnO_2 nanocomposites	102
4.27	The variation of resistance as a function of temperature of PAni/CuO nanocomposites	102
4.28	Plot of ln(σ) vs. 1000/T of PAni NFs, SnO_2 and CuO thin films	104
4.29	Plot of ln(σ) vs. 1000/T of PAni/SnO_2 nanocomposites thin films	104
4.30	Plot of ln(σ) vs. 1000/T of PAni/CuO nanocomposites thin films	105
4.31	The variation of capacitance versus reverse bias voltage for PAni NFs, SnO_2 and CuO thin films	107
4.32	The variation of capacitance versus reverse bias voltage for PAni/SnO_2 nanocomposites thin films	108
4.33	The variation of capacitance versus reverse bias voltage for PAni/CuO nanocomposites thin films	108

4.34	The variation of $1/C^2$ versus reverse bias voltage for of PAni NFs, SnO_2 and CuO thin films	109
4.35	The variation of $1/C^2$ versus reverse bias voltage for of PAni/SnO_2 nanocomposites thin films	110
4.36	The variation of $1/C^2$ versus reverse bias voltage for of PAni/CuO nanocomposites thin films	110
4.37	I-V characteristics in the dark and under light with different intensities for PAni NFs thin films	111
4.38	I-V characteristics in the dark and under light with different intensities for SnO_2 thin films	112
4.39	I-V characteristics in the dark and under light with different intensities for CuO thin films	112
4.40	I-V characteristics in the dark and under light with different intensities of 10mL PAni- 3 mL SnO_2 thin films	113
4.41	I-V characteristics in the dark and under light with different intensities of 10mL PAni- 5 mL SnO_2 thin films	113
4.42	I-V characteristics in the dark and under light with different intensities of 10mL PAni- 7 mL SnO_2 thin films	114
4.43	I-V characteristics in the dark and under light with different intensities of 10mL PAni- 3 mL CuO thin films	114
4.44	I-V characteristics in the dark and under light with different intensities of 10mL PAni- 5 mL CuO thin films	115
4.45	I-V characteristics in the dark and under light with different intensities of 10mL PAni- 7 mL CuO thin films	115
4.46	I-V characteristics in the dark for PAni NFs	117
4.47	Photoresponse time of the fabricated PAni NFs UV photodetector upon exposure to (250, 300, 350, 400 and 500) nm	119
4.48	Photoresponse time of the fabricated SnO_2 nanostructures and PAni/SnO_2 nanocomposite with different SnO_2 contents UV photodetector upon exposure to (250, 300, 350 and 400) nm	120
4.49	Photoresponse time of the fabricated CuO and PAni/CuO nanocomposite with different CuO contents UV photodetector upon exposure to (250, 300, 350 and 400) nm	120
4.50	The variation of spectral responsivity with wavelength for (a) PAni NFs (b) SnO_2 and its composites with PAni (c) CuO and its composites with PAni	123
4.51	The variation of photocurrent Gain (G) with wavelength for (a) PAni NFs (b) SnO_2 and its composites with PAni (c) CuO and its composites with PAni	124
4.52	The variation of NEP with wavelength for (a) PAni NFs (b) SnO_2 and its composites with PAni (c) CuO	125

	and its composites with PAni	
4.53	The variation of detectivity with wavelength for (a) PAni NFs (b) SnO_2 and its composites with PAni (c) CuO and its composites with PAni	126
4.54	The variation of specific detectivity with wavelength for (a) PAni NFs (b) SnO_2 and its composites with PAni (c) CuO and its composites with PAni	127
4.55	The variation of resistance with time for PAni NFs thin films as H_2S gas sensor at different operating temperatures	129
4.56	The variation of resistance with time for SnO_2 thin film as H_2S gas sensor at different operating temperatures	129
4.57	The variation of resistance with time for CuO thin film as H_2S gas sensor at different operating temperatures	130
4.58	The variation of resistance with time for 10 mL PAni – 3 mL SnO_2 thin film as H_2S gas sensor at different operating temperatures	130
4.59	The variation of resistance with time for 10 mL PAni – 5mL SnO_2 thin film as H_2S gas sensor at different operating temperatures	130
4.60	The variation of resistance with time for 10mL PAni – 7 mL SnO_2 thin film as H_2S gas sensor at different operating temperatures	131
4.61	The variation of resistance with time for 10 mL PAni – 3 mL CuO thin film as H_2S gas sensor at different operating temperatures	131
4.62	The variation of resistance with time for 10 mL PAni – 5 mL CuO thin film as H_2S gas sensor at different operating temperatures	131
4.63	The variation of resistance with time for 10 mL PAni – 7 mL CuO thin film as H_2S gas sensor at different operating temperatures	132

List of Symbols

Symbol	Meaning	Unit
θ	Diffraction Angle	Degree
t	Thickness	nm
hkl	Miller Indices	
k_B	Boltzmann's Constant	J/k
$h\nu$	Photon Energy	eV
α	Absorption Coefficient	cm^{-1}
A' and γ	Constants Depending on Properties of Conduction and Valance Bands	
υ	Frequency	Hz
K_e	Wave Vector of Transmitted Electron	cm^{-1}
$\vec{K}_{ph}$	Photon Wave Vector	cm^{-1}
$\vec{K}$	Wave Vector	cm^{-1}
M	The Molar Concentration	mol/L
M_{wt}	Molecular Weight	g/mol
V	Volume of Distilled Water	mL
a	Lattice Constant	Å
b	Lattice Constant	Å
c	Lattice Constant	Å
FWHM(**β**)	Full Width at Half Maximum	rad
D_{av}	Average Crystallite Size	nm
d_{hkl}	Interplanner Spacing	Å
S	Micro Strain	%
λ	Wavelength	Å
N_0	Number of Grains Per Unit Area	cm^{-2}
δ	Dislocation Density	Line. cm^{-2}
E_g	Energy Band Gap	eV

E_u	Urbach Energy	meV
E_d	Dispersion Energy	eV
E_v	Valence Band Energy	eV
E_c	Conduction Band Energy	eV
E_p	Assistant Phonon Energy	eV
λ_C	Cut off Wavelength	nm
h	Planck's Constant	J.s
J	Current Density	A/cm^2
T	Transmittance	
A	Absorbance	
μ_n	The Mobility of Electron	$cm^2/V.s$
μ_p	The Mobility of Hole	$cm^2/V.s$
τ	Carrier's Lifetime	s
V_d	The Drift Velocity	m/s
m*	The Effective Mass	g
Σ	The Electrical Conductivity	$(\Omega.cm)^{-1}$
σ_o	The Minimum Electrical Conductivity at 0 K	$(\Omega.cm)^{-1}$
E_a	The Activation Energy	eV
B	Magnetic Field	Tesla
R_H	The Hall Coefficient	cm^3/C
V_H	The Hall Voltage	Volt
μ_H	The Hall Mobility	$cm^2/V.s$
V_{bi}	The Built - In Voltage	Volt
q or e	The Electron Charge	C
n	The Carrier Concentration	cm^{-3}
p	The Hole Concentration	cm^{-3}
I_o	The Saturation Current	A

A*	The Effective Richardson Constant	$A.m^{-2}K^{-2}$
T	The Absolute Temperature	K
Φ_B	The Barrier Height	eV
n	The Ideality Factor	
$\mathbf{A_t}$	Tunneling Constant	
V_F	The Forward Bias Voltage	Volt
I_F	The Forward Bias Current	A
τ_r	Rise Time	s
τ_f	Fall Time	s
Δf	Bandwidth	Hz
R_λ	Responsivity	A/W
$J_{ph}(\lambda)$	The Photocurrent Density From the Tested Detector	A/cm^2
$P_{inc}(\lambda)$	The Incident Power Density	μw/cm
c	The Speed Of Light	m/s
NEP	Noise-Equivalent Power	W
I_n	I_n Noise Current	A
R_d	Dark Resistance	Ω
D	Detectivity	W^{-1}
D^*	Specific Detectivity	$(cm\ Hz^{1/2}\ W^{-1})$.
S	Sensitivity	
R_a & R_g	R_g The Electrical Resistance of the Film in The Air and Electrical Resistance	Ω

List of Abbreviations

Symbol	Meaning
0D	Zero Dimensions
1D	One Dimensions
2D	Two Dimensions
3D	Three Dimensions
DOS	Density Of States
CT	Charge Transfer
PAni NFs	Polyaniline Nano Fibers
FET	Field-Effect Transistors
PCBs	Printed Circuit Boards
OIHC	Organic-Inorganic Hybrid Composite
MOF	Metal Organic Frameworks
NBB	Nano Building Blocks
LEDs	Light Emitting Diodes
UV-Vis	Ultra Violet Visible
IR	Infrared
FTIR	Fourier Transform Infrared Spectroscopic
XRD	X- Ray Diffraction
FESEM	Field Emission Scanning Electron Microscopy
TEM	Transmission Electron Microscopy
SPM	Scanning Probe Microscopy
D.C	Direct Current
A.C	Alternating Current
CV	Capacitance –Voltage
PC	Photoconductivity
I-V	Current-Voltage
RT	Room-Temperature
PL	Photoluminescence
MRS	Micro-Raman Scattering

NPs	Nanoparticles
IPCE	The Incident Photon-To-Current Efficiency
CSA	Camphor Sulfonic Acid
CTAB	Cetyltrimethylammonium Bromide
SAED	Selected Area Electron Diffraction
C.B	Conduction Band
V.B	Valance Band
W-H	Williamson-Hall
FAP	Fundamental Absorption Process
SRO	Short Range Order
SPR	Surface Plasmon Resonance
VOCs	The Detection of Volatile Organic Compounds
SDS	Sodium Dodecyl Sulphate

Chapter One

Introduction and Basic Concept

1.1 Introduction

One goal of today's technology is the miniaturization of the electronic, actuating, sensing, and optical devices and their components; hence, nanotechnology is an advanced technology that has received a lot of attention from the world of the science and industry for its ability to make use of the unique properties of nanosized materials. Nanotechnology is capable of manipulating and controlling material structures at the nano level (a nanometer equals to one millionth of a millimeter) and offering unprecedented functions and excellent material properties [1]. Nanotechnology can be defined as the ability to work near the molecular level, atom by atom, to create large structures with fundamentally new properties and functions. Nanotechnology can be described as the precision-creation and precision control of atomic-scale matter [2]. It offers new design, characterization, production, and application of systems, devices and materials at the nanometer scale. It is an interesting and vibrant field of research. Their roots can be traced back to Feynman's famous lecture in 1959, in which he suggested that for entities with nanoscopic dimensions new physical phenomena should arise [3]. The nanoscale dimension is important because quantum mechanical properties of electronics, photons, and atoms are evident at this scale. Its structures permit the control of fundamental properties of materials without changing the materials' chemical status. Nanostructures, such as nanophotonic devices, nanowires, carbon nanotubes, plasmonic devices, among others, are planned to be more powerful communication systems and quantum computers [4].

Nanoscale structures are used to study a range of interesting effects that occur when electrons are confined to very small geometries. For example, the quantized electron wave states in a nanostructure are reflected in measurements of electron transport through the structure. Electron transport experiments have been used to investigate many different

nanostructures. As the scale of materials is reduced to nanometers, the tendency of surfaces to minimize their free energy may drive structural changes [5].

1.2 The Physics of Low Dimensional Material

Over the last few years, advances in solid state physics have been characterized by a change from bulk crystal to a very small at least one of their three dimensions. Semiconductor nanocrystals are the subject of a rapidly developing field. It can be defined as crystals with dimensions ranging from 1-100 nm; above this size, they are termed microcrystals. When the dimensions of a solid are reduced from a large size to the size of the characteristic lengths of electrons i.e. de Broglie wavelength λ_B, coherence length and localization length then the particles behave wave-like and the crystal size becomes smaller leading to the semiconductor energy levels to be more separated from each other and the effective band gap to increase, therefore new physical properties due to quantum effect is observed, such as: quantum conductance oscillations, quantum Hall effects, resonant tunneling single electron transport, etc. These properties are necessary to build nanostructure semiconductor heterojunction, super lattice, etc. [6].

Low dimensions materials are classified according to the number of dimensions in nanometer size into three types [7]: **Quantum wells (2D), Quantum wires (1D), and Quantum dots (0D).**

1.3 Conducting polymers

The term “polymer” comes from “poly”, which means many, and “mer”, which means units. Conducting polymers are a prospective class of new materials that combine solubility, process ability and flexibility of plastics with electrical and optical properties of metals and semiconductors [8].

1.4 Conjugated Polymer

A polymer chain is characterized by an alternation of saturated and unsaturated carbon-carbon bonds, leading to the presence of non-localized electrons {π–electrons} [9]. The conjugated structure with alternating single and double bonds or conjugated segment coupled with atoms providing P-orbital for a continues orbital overlap seem to be necessary for polymers to become electrically conducting. This is due to the conjugated structure not only provides a continues conduction path through the P-orbital overlapping along the polymer backbone but also facilitates the generation of charge carriers by either partial oxidation (p-doping) or partial reduction (n-doping) [10,11]. For the last three decades, a large effort has been carried out on the development of conducting polymers such as Polythiophene (PT), Polypyrrole (PPy), polyphenylene (PP), polyphenylene vinylene (PPV), polyasulfone (PS), and polyaniline (PAni) [12,13]. Figure (1.1) shows the chemical structural formula of some commonly encountered conjugated polymers [14].

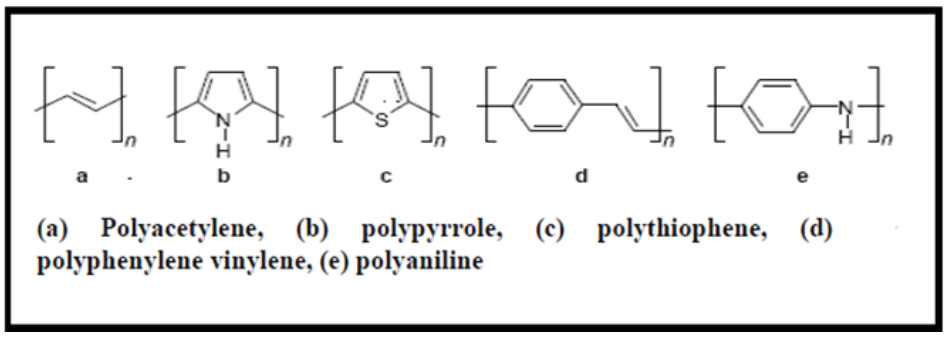

(a) Polyacetylene, (b) polypyrrole, (c) polythiophene, (d) polyphenylene vinylene, (e) polyaniline

Figure 1.1: Intrinsically conducting polymers [14].

These polymers because of their good electrical and optical properties have been applied in a really impressive application range in different fields such as energy storage electromagnetic interference shielding [15], light emitting diodes and photovoltaic devices, field effect transistors, plastic lasers, batteries, corrosion protection and chemical and biological sensors [16, 17].

1.5 Polyaniline (PAni)

Polyaniline (C_6H_7N) has been known for more than a century in its "aniline black" form. Among the conducting polymers, polyaniline is the most promising polymer due to its low cost, chemical stability [18], controllable electrical conductivity, excellent environmental stability, ease to synthesize through chemical or electrochemical processes and have many interesting characteristics for sensing including their high sensitivity and short response time. PAni is represented by the general following formula and structure, where B denotes a benzoid reduced unit and Q is aquinoid oxidized unit [19] as shown in Figure (1.2)

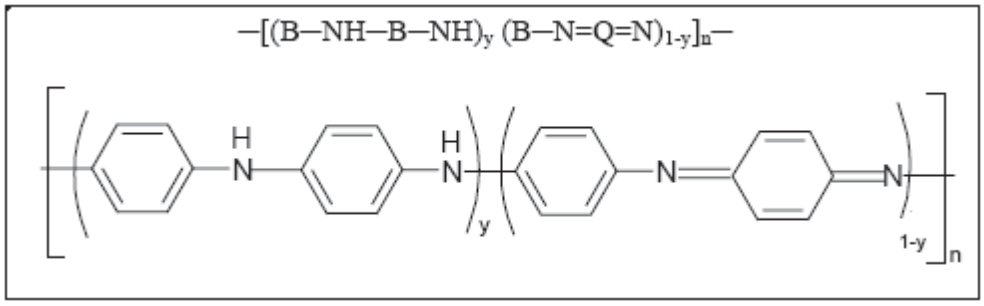

Figure 1.2: Structure of the polyaniline chain [20].

PAni is a typical phenylene-base polymer having a chemically flexible -NH – group in the polymer chain flanked on either side by a phenylene ring. The protonation, deprotonation and various other physico-chemical properties of PAni can be traced to the presence of the –NH- group [21]. PAni exists in various oxidation states characterized by the ratio of amine to imine nitrogen atoms [22]. When y = 1, the polymer is in the fully reduced leucoemeraldine (LE) state and is found to be insulating and yellow. The half oxidized polymer (y=0.5) is called emeraldine base (EB) and is insulating and blue. The only conducting state of PAni is the green colored emeraldine salt (ES), which is protonated form of EB [23]. Finally, pernigraniline base (PN) is the fully oxidized form of PAni (Y= 0) and is

insulating and purple. All these oxidation states of PAni are shown in Figure (1.3) [24].

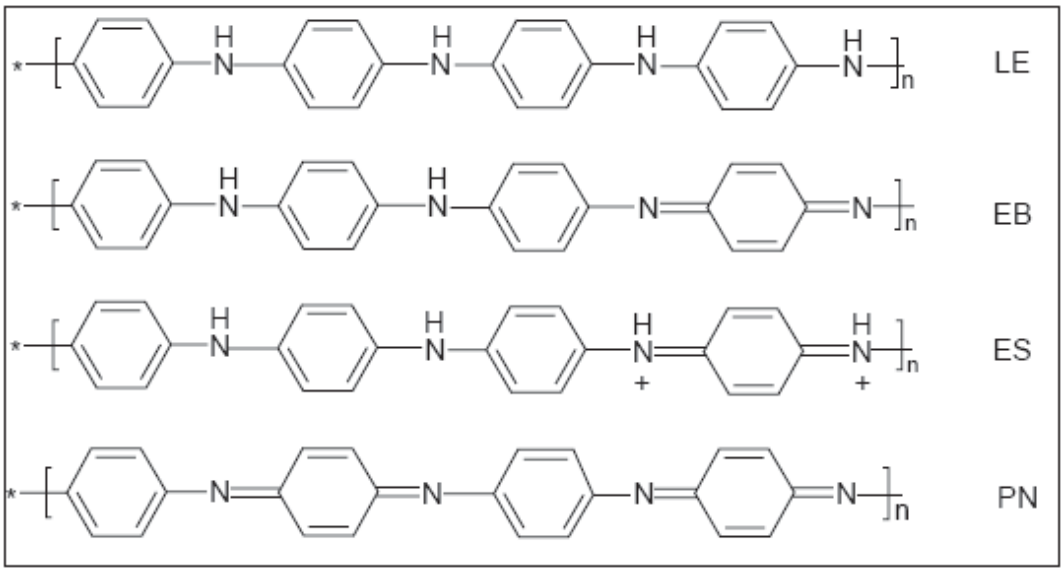

Figure 1.3: Different oxidation states of PAni, leucoemeraldine (LE), emeraldine base (EB), emeraldine salt (ES) and pernigraniline (PN) [24].

The ability of PAni to exist in various forms via acid/base treatment and oxidation /reduction, either chemically or electrochemically, has made PAni the most tunable member of the conducting polymer. PAni was found in wide variety of applications in different fields [25]. However, PAni has a rigid backbone originating from an extended conjugated double bond [26]. The rigid structure of PAni restricts its common usage and results in the insolubility, infusibility and incompatibility of this material with common polymers. This necessitates the modification of the structure of PAni. Therefore, during the past decade researchers have directed their attention to modify PAni structure and to overcome the difficulties associated with the use of PAni by using different approaches, for example, the utilization of a soluble precursor method, in which a process able precursor polymer is first prepared in an appropriate form and then chemically converted into the final conducting polymer [27]. Another approach is the formation of conductive blends/composites [28] or the formation of PAni filled interpenetrating polymer networks. Efforts have been made to improve the properties of

PAni through the post treatment of PAni such as sulfonation or incorporation of N-alkyl sulfonic acid pendant group (the use of functional dopants and the design of self-doping polymer) [29]. Extensive studies on the polymerization of aniline (Ani) derivatives and/or the polymerization of Ani in the presence of another monomer (copolymerization) have also been carried out frequently in order to improve the properties of PAni. In recent years, due to the development of nanotechnology, PAni has been employed for studying nano composite materials in order to get new desired properties for practical application [30].

1.5.1 Different oxidation states of PAni

Unlike other known electro conducting polymers, polyaniline can exist, depending on degree of oxidation, in different forms known as: leuoemeraldine, emeraldine and perningraniline. Leuoemeraldine base refers to fully reduced form; emeraldine base is half-oxidized, while perningraniline base is completely oxidized form of polyaniline. The only conducting form of polyaniline is emeraldine salt, obtained by doping or protonation of emeraldine base [31, 32]. The unique feature of mentioned polyaniline forms is ease of its mutual conversions by both chemical and electrochemical reactions as it can be seen in Figure (1.4) [33]. Apart from the changes in oxidation levels, all the transitions among polyaniline forms are manifested by color and conductivity changes [33]. The conducting protonated emeraldine in the form of green emeraldine salt, obtained as a product of electrochemical polymerization of aniline in acidic electrolytes, can be easily transformed by further oxidation to fully oxidized dark blue perningraniline salt, which can be treated by alkali to form violet perningraniline. Emeraldine salt can also be reduced to transparent leuoemeraldine, or can be transformed by alkali to blue non conducting emeraldine. The two blue forms of polyaniline, perningraniline salt and

emeraldine have different shades of blue [33]. Both, reduction of emeraldine salt to leuoemeraldine and oxidation to perningraniline states are followed by decrease in conductivity [34].

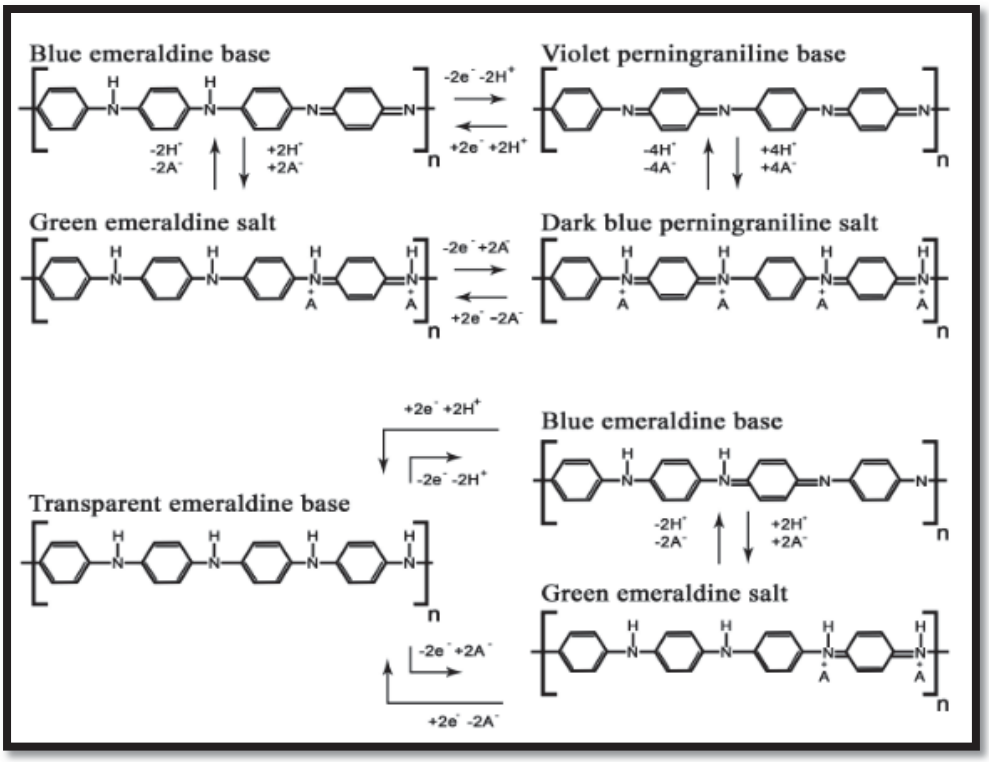

Figure 1.4: Different forms of polyaniline [33].

1.5.2 Polyaniline Conductivity

The mechanism of polyaniline conductivity differs from other electro conducting polymers, owing to the fact that nitrogen atom is involved in the formation of radical cation; unlike most of the electro conducting polymers whose radical cation is formed at carbon. On the other hand, nitrogen is also involved in the conjugated double bonds system. Therefore, electrical conductivity of polyaniline is dependent both on the oxidation and protonation degrees [35]. As mentioned before, polyaniline is characterized by existence of various oxidation forms. Polyaniline in the form of emeraldine base can be doped (protonated) to conducting form of emeraldine salt. Emeraldine base, half oxidized form, is consisted of equal amount of amine (-NH-) and imine (=NH-) sites. Imine sites are subjected

to protonation to form bipolaron or dication (emeraldine salt form). Bipolaron is further dissociated by injection of two electrons both from electron pairs of two imine nitrogen, into quinoid imine ring, and the third double bond of benzenoid ring is formed [34]. Unpaired electrons at nitrogen atoms are cation radicals, but essentially they represent polarons. Figure (1.5) represents the polaron lattice, responsible for high conductivity of polyaniline in the form of emeraldine salt formed by redistribution of polarons along polymer chain [35].

Although both bipolaron and polaron theoretical models of emeraldine salt conductivity were proposed [36], it was lately confirmed that, beside from the fact that few of spineless bipolarons exist in polyaniline, formation of polarons as charge carriers explained high conductivity of polyaniline. Unique property of polyaniline is conductivity dependence on the doping (proton) level [35].

The maximum conductivity of polyaniline is achieved at doping degree of 50%, which corresponds to polyaniline in the form of emeraldine salt [37]. For higher doping degrees some of the amine sites are protonated, while lower doping degrees, i.e. some of the imine sites, were left un protonated [35], explaining why, in the light of the polaron conductivity model, reduction of emeraldine salt to leuoemeraldine and oxidation to perningraniline states decrease the conductivity. The order of conductivity magnitude varies from 10^{-2} S cm^{-1} for un doped emeraldine, up to 10^{3} S cm^{-1} for doped emeraldine salt [38].

Beside the fact that doping degree has the pronounced effect on the conductivity, other factors such as: moisture amount, morphology, temperature etc. were also found to have influence on the polyaniline conductivity[39, 40].

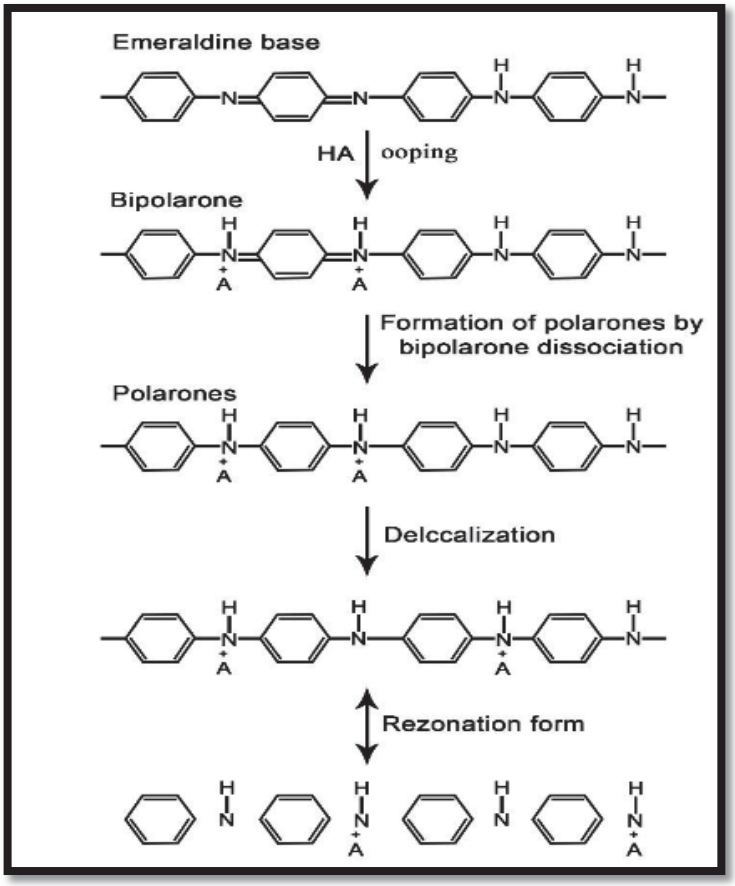

Figure 1.5: Schematic presentation of conductivity for polyaniline [35].

1.6 Applications of conducting polymers

Basic research and assessment of possible applications of conducting polymers all over the world show that this area is interdisciplinary in nature. Variety of technology oriented applications of conducting polymers includes electronics, optoelectronics, solar cells, semiconductors, laser, energy storage and super capacitors fields [41]. Some of these applications are as follows: Conducting organic molecular electronic materials have attracted much attention because of their many projected applications in solar cells, light weight batteries, electrochromic devices, sensors and molecular electronic devices. Polymeric heterojunctions and solar cells have been fabricated using PPy on silicon via electrochemical methods. Conducting polymers such as polyacetylene, PAni, PPy, Polythiophene, polyindole, etc. have been emerged as electrode materials in rechargeable

batteries. PPy films are applied in neurotransmitter as a drug release system into the brain. Conducting polymers have been used to fabricate diodes, capacitors, field-effect transistors (FET) and printed circuit boards (PCBs) in the field of electronics and photonics. PAni is being used as anti-static coating material for electronic storage devices, electronic boards, sensors, appliances etc. Biosensors have found promising applications in various fields such as biotechnology, food and agriculture product processing, health care, medicine and pollution monitoring [42].

1.7 Hybrids of conducting polymers

1.7.1 Introduction of Hybrids

Organic-inorganic hybrid composite (OIHC) materials are defined as "the solid materials' composites with organic and inorganic components intimately mixed where at least one of the components domains has a dimension ranging from few angstroms to several nanometres". Hybrid materials are defined as "mixtures of two or more materials with new properties created by new electron orbitals formed between such materials. Yamada et al. defined hybrid materials as "mixtures of two or more materials with newly formed chemical bonds" [43,44]. Hybrid materials play a major role in the development of advanced functional materials. Inorganic materials have good mechanical and thermal stability as well as optical properties; however they are hard, and brittle. Organic polymers/oligomers are flexible and generally suffer from instability to heat and tendency of natural degradation upon aging. Nevertheless, upon forming hybrid material with inorganic component, the organic moiety would provide flexibility, toughness, hydrophobicity and new electronic and/or optical properties. In principle, modification of the kind and proportions of the constituents allows an intentional tailoring of properties evolving from organic and inorganic materials [45]. Thus OIHC materials

could have desired and new features which may not be present in individual organic and inorganic components [46].

1.7.2 Classification of hybrid materials

Hybrid materials are classified into Class I and Class II based on the criteria of their chemical nature. In Class I hybrid materials, organic and inorganic components are dispersed and held together only by weak forces such as van der Waals interactions. In Class II hybrid materials, the organic and inorganic moieties are linked through strong bonds such as covalent bonds [47]. The hybrid and their related materials can be categorized into four types as follows [44]:

1. **Composites**: Mixture of materials consisting of matrix constituents at micrometer to millimeter level dispersion.

2. **Nanocomposites**: Mixture of similar kinds of materials at submicron and nano level.

3. **Hybrids**: Composites consisting of two constituents at the nanometer or molecular level.

4. **Nanohybrids**: Mixture of different materials with chemical bonds between their different materials at atomic or molecular level.

Classification of materials on the basis of different scale levels as in Figure (1.6) [48].

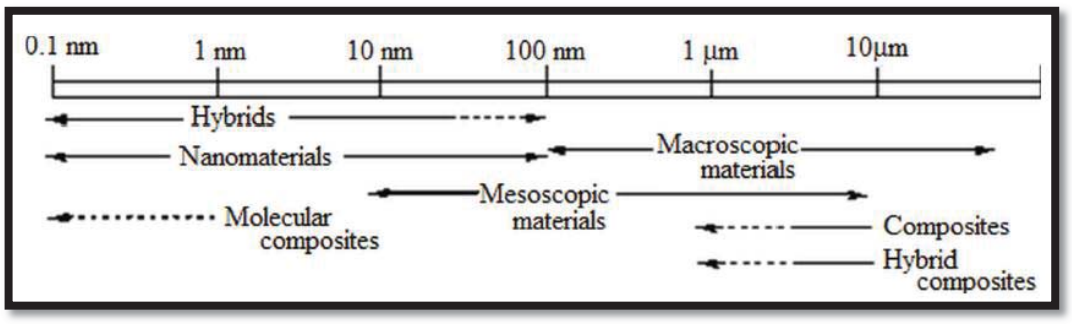

Figure 1.6: Classification of materials at different scale levels [48].

1.7.3 Factors influencing properties of hybrid materials

The properties of a composite product depend not only on the properties of the individual components, but also on factors such as the phase's size, shape and interfacial properties [49]. In fact, the inner surfaces predominantly play a role in deciding the properties of these hybrid materials. If the dimensions of one or both phases involved in the composite material are reduced down to the nanometer scale or even the molecular level, a synergic combination of both the constituents is possible. Properties of such nanocomposites will be different from that of classical composites, since many properties correlate with the phase dimension. Figure (1.7) depicts composites and hybrids with dimension and phases. Mixing the constituents at the microscopic scale leads to a more homogeneous material. The characteristics of this material lie either between the two original phases or even in newer properties [43].

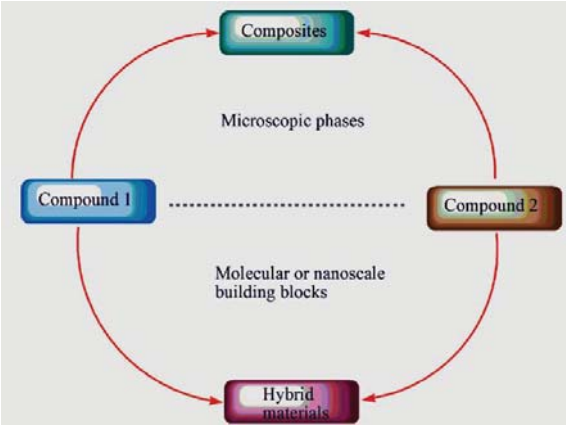

Figure 1.7: Composites and hybrids with phases[44]

1.7.4 Synthesis of hybrid materials

There are few methods commonly used for the synthesis of hybrid materials [50]. These methods are:

1. Hydrothermal synthesis

2. Sol-gel synthesis

3. Encapsulation

4. Impregnation etc.

Hydrothermal method has been employed to grow organic, inorganic and organic –inorganic nanostructures. The hydrothermal technique is one of the most important methods for advanced materials processing, particularly owing to its advantages in the processing of nanostructured materials with a control over size and morphology properties for a wide variety of technological applications such as electronics, optoelectronics, catalysis, ceramics, magnetic data storage, biomedical, biophotonics, etc. The hydrothermal technique not only helps in processing mono dispersed and highly homogeneous nanoparticles, but also acts as one of the most attractive techniques for processing nano-hybrid and nanocomposite materials. Hydrothermal processing can be defined as any heterogeneous reaction in the presence of aqueous solvents or mineralizers under high pressure in a closed system and temperature conditions to dissolve and recrystallize (recover) materials that are relatively insoluble under ordinary conditions. Definition of the word hydrothermal has undergone several changes from the original Greek meaning of the words ‘hydros’ meaning water and ‘thermos’ meaning heat [51]

Sol-gel method is simple, low cost and yields amorphous nanocomposite hybrid materials. Hydrolysis of organically modified metal alkoxides/metal halides with/without simple metallic alkoxides in presence/absence of a specific cross linking agent yields the hybrid materials. Interactions such as hydrogen bonds, π - π interactions, van der Waals forces etc. are found between organic and inorganic components in the hybrid materials. These materials exhibit infinite microstructures and are easily shaped as films or bulks. They are generally poly dispersed in size

and locally heterogeneous in chemical composition.

In encapsulation technique, organic components get trapped during hydrolysis and condensation reactions of metal alkoxides and/or organosilanes. Organic molecules, oligomers, macromonomers and bio-components can be easily incorporated into metal oxide-based networks. This method provides heterogeneity to the organic components and thus increases life time and reuse of such precious organic components.

In impregnation method, organic components are introduced inside the porous network. Both encapsulation and impregnation methods have been extensively developed either by inorganic sol-gel chemists or by polymer chemists. Inorganic structures like silica, titania (TiO_2) and other metal oxides can function as host matrix. These amorphous composites with the control of their microstructure, exhibit a wide variety of mechanical, optical, electrical, ionic, sensor, catalytic properties [52].

1.7.5 Applications of hybrid materials

Hybridization of conducting polymers with inorganic materials has been found to improve the inherent properties of both organic and inorganic components. Thus, they open promising applications in many areas: optics, electronics, ionics, mechanics, energy, environment, biology and medicine. They are finding very high position in photovoltaic and fuel cells, photo catalysts, new catalysts, chemical/biomedical sensors, smart micro-electronic, micro-optical and photonic components etc. The practical applications of hybrid materials are many and few are listed below [53, 54]:

a) Decorative coatings by making use of organic dyes in hybrid coatings.

b) Scratch resistant coatings with hydrophobic or antifogging properties.

c) Electronic and optoelectronic applications like light emitting diodes,

photodiodes, solar cells, gas sensors and field effect transistors.

d) Fire retardant materials for building construction industries.

e) Filling materials in dental treatment.

f) Electrolyte materials in solid state lithium batteries or super capacitors.

g) Antistatic / antireflection / anti corrosion coatings.

h) Porous hybrid materials for adsorption and catalytic applications.

1.8 Tin Oxides

Tin oxide (SnO_2) is a tetragonal rutile structure with lattice parameters a=b = 4.737 Å and c = 3.826 Å [55]. The unit cell contains two tin and four oxygen atoms. Each tin atom is bounded to six oxygen atoms at the corners of a regular octahedron, and every oxygen atom is surrounded by three tin atoms at the corners of an equilateral triangle as shown in figure (1.8) [56].

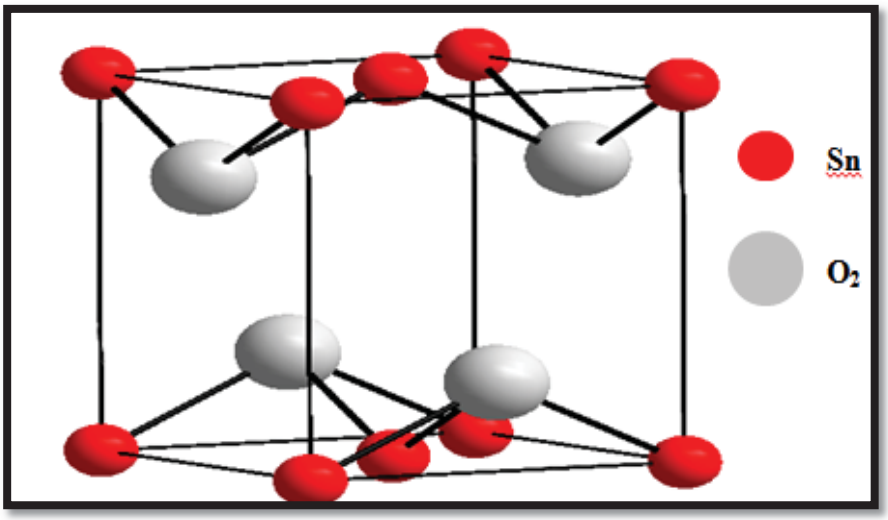

Figure 1.8: The lattice structure of SnO_2 [56].

The SnO_2 films are n-type semiconductors with a direct band gap of about (3.6- 4.3) eV. Deposition technique has strong effect on the thin film form and its structure, so it may be formed as polycrystalline or amorphous. SnO_2 semiconducting transparent thin films have various appealing features

for technical applications in solar energy conversion, flat panel displays, electrochromic devices, invisible security circuits, LEDs, gas sensing, etc. Hence large area SnO_2 films on cheap and easily available substrates are of considerable interest for the formation of most of the photonic structures [57]. Table (1.1) shows the properties of SnO_2.

Table 1.1: The properties of SnO_2 [56].

Lattice constants	a=b= 4.737 (Å), c= 3.826 (Å)
Density	6.95 (g / cm^3)
Melting point	1630 (°C)
Appearance	White powder
Crystal structure	Rutile (tetragonal)
Molecular weight	150.69 (g/mol)
Type of conductivity	n-type

1.9 Copper oxide

Copper oxide has types of polymorphism, namely, cuprous oxide (Cu_2O) and cupric oxide (CuO). These oxides are the two most important stoichiometric compounds in the Cu-O system. Both oxides are intrinsic p-type semiconductor with relatively small band gaps and show many attractive properties that can be utilized in diversity on applications. The potential applications of copper oxides include solar cells [58] Li-ion battery where they have been used as negative electrode material, superconductor, magnetic storage, gas sensors and photo-conductive

systems [59].

Cupric oxide (CuO) is an intrinsic p- type semiconductor with a band gap in the range of (1.2 -1.58) eV. The CuO has a C_2/c monoclinic crystal structure as shown in Figure (1.9) [60]. The unit cell of CuO comprises Cu^{+2} ions which are coordinated by four O^{-2} ions in an approximately square planar configuration. The abundance of its source material (Cu) together with other features such as low cost production, good thermal stability, and electrochemical properties make CuO a promising material in various applications. Furthermore, the iconicity of the Cu-O bands increases when the size of the material approached the nanodomain. This property combined with relatively large aspect ratio of CuO nanomaterials that is very attractive for applications such as gas sensing and catalyst for degradation of hazardous chemicals. Some of the important properties of CuO bulk material are given in Table (1.2).

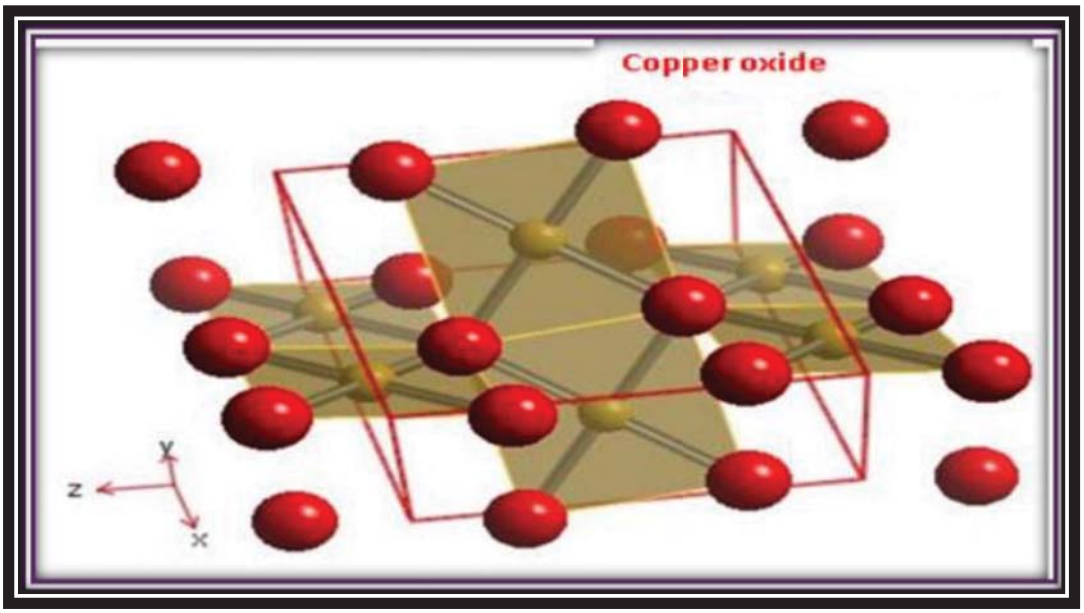

Figure 1.9: The lattice structure of CuO [61].

Table 1.2: The properties of CuO [62].

Lattice constants	a = 0.468, b= 0.342 ,c= 0.513 (nm)
Density	6.31 (g / cm^3)
Melting point	1975 (°C)
Crystal structure	Monoclinic
Appearance	Black Powder
Molar mass	79.545 g/mol
Type of conductivity	p-type

1.10 Thin Films

The term "Thin Films" is used to describe a layer or several layers of atoms of a certain substance whose thickness ranges between (10 nm) and less than 1μm (1000 nm) [63]. Thin films technique is one of the most recent fully grown technologies that greatly contribute to develop the study of semiconductors and metals by giving a clear indication of their chemical and physical properties. The properties of thin films are usually different from those of the bulk because of the two dimensions nature of thin films. In bulk “three dimensions” the particles are under the influence of forces at all directions, while in thin films the forces act upon the particles at the surface only [64]. Thin films are first made by (Buser & Grove) in 1852 by using (Chemical Reaction) and later in 1857; the scientist (Farady) obtained a thin metal film by means of (Thermal Evaporation) [65]. Spray pyrolysis was first used commercially in 1947 as in U.S. patents registered for (H. A. McMaster and W. O. Lytle) to deposit conductive oxide films on heated glass substrate [66 , 67]. The film layer is deposited on certain plates chosen according to the nature of the study or the scientific need. Such plates could

be glass slides, silicon wafers, aluminum, quartz and others [63].

There are already so many applications of thin films such as the electronic and optical applications**.** The applications of thin films in electronics have been grown steadily in importance during the last decades, because of their use in the electronic resistances, capacitances, transistors, integral circuits for digital computers and other electronic equipments. Thin films are also particularly important for their use in great number of optical fields such as the manufacturing of ordinary and thermal mirrors, mirrors for high reflectance, semitransparent reflection coating which are used in optical devices such as filters in solar cells, and non-absorbing materials which are used for interference phenomena [67].

1.11 Thin Films Deposition Techniques

Thin films deposition techniques can be divided essentially into two main groups, namely, physical and chemical techniques [68, 69]. These techniques are shown in Figure (1.10).

1.11.1 Spin Coating Technique

Spin coating is the most widely used deposition chemical technique for the development of organic or in organic sensing so far. Highly reproducible as well as very homogenous films can be deposited by this technique. Two forces are acting on the solution during spin coating; the adhesive forces at the solution substrate interface and the centrifugal forces resulting from the high-speed rotation. These two competing forces will result in a strong shearing action at the interface which causes the solution to form a thin film with controllable thickness, depending on angular velocity, solution concentration and viscosity [70]. To get homogeneous films, several different factors are important and have to be considered such as evaporation rate of the solvent, viscosity of the fluid, concentration of the

solution, angular velocity (rotating speed) and spinning time.

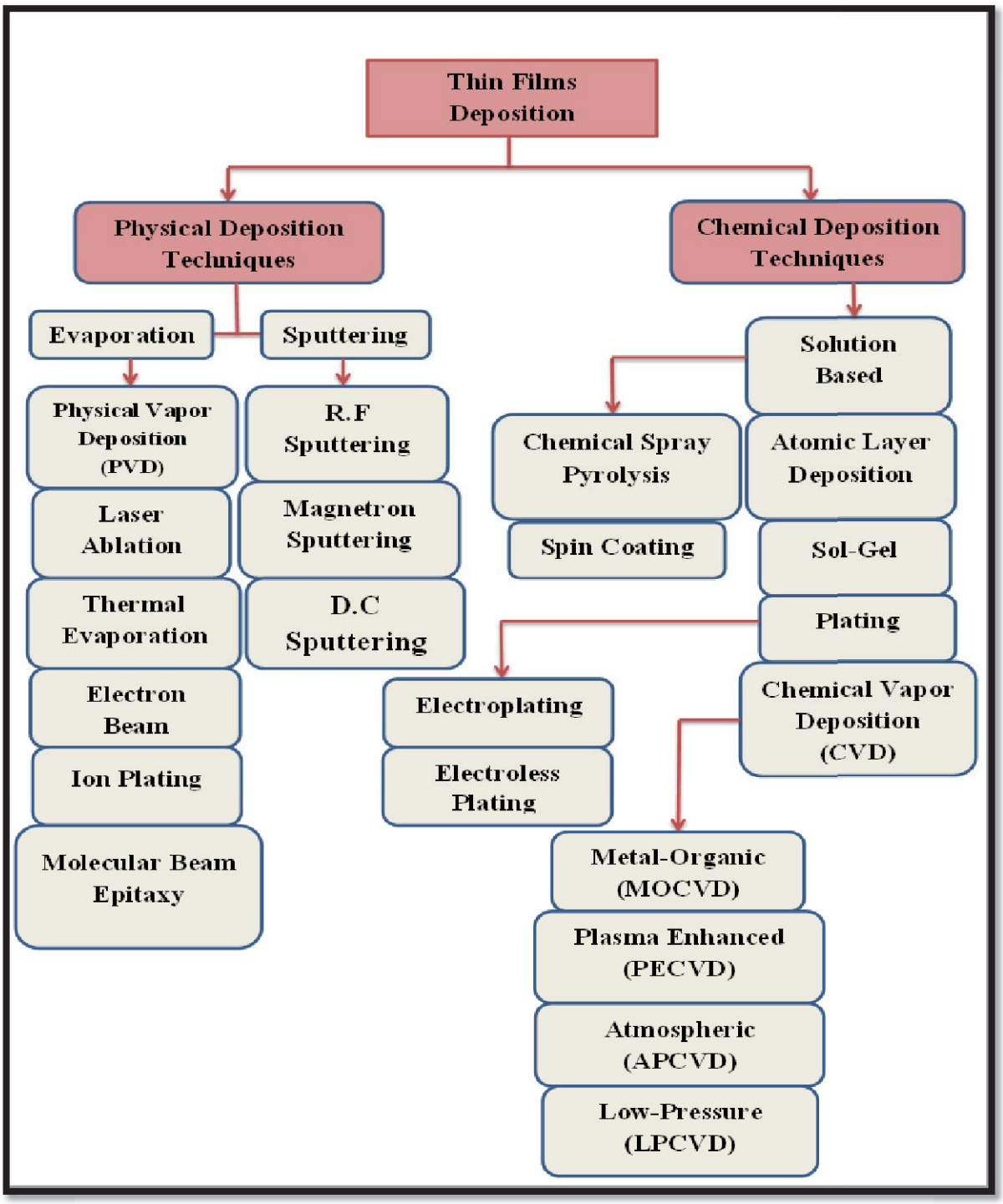

Figure 1.10: Classification of thin film deposition techniques [69].

1.12 Previous Studies

In **(2004), Bubb et al.** deposited conducting polyaniline thin films by a laser-based vaporization technique. The films have been characterized by

infrared spectroscopy, UV-Vis spectroscopy, four-point conductivity measurements, thermo gravimetric analysis, and fluorescence measurements. In addition, the films have been characterized with respect to their photoconductive response to 532nm laser light. It is found that the films exhibit persistent photoconductivity and it is proposed that defect base sequences may be responsible for the charge localization that results in such a photoconductive response [71].

In **(2007), Geng et al.** prepared a polyaniline (PAni)/SnO_2 hybrid material by a hydrothermal method and the XRD pattern suggested that PAni did not modify the crystal structure of SnO_2, but SnO_2 affected the crystallization of PAni to some extent. The gas sensitivity of the PAni/SnO_2 hybrid was also studied to ethanol and acetone at operation temperatures of 30, 60 and 90 ^oC. It was found that the PAni/SnO_2 hybrid material had gas sensitivity only when operated at 60 and 90 ^oC, and it showed a linear relationship between the responses and the concentrations of ethanol and acetone at 90 ^oC [72].

In **(2010), Abdolahi et al.** prepared chemically polyaniline nanofibers by an interfacial polymerization. Ammonium persulfate, hydrochloric acid and chloroform were used as oxidant, dopant and organic solvent respectively. FESEM results show that polyaniline has nanofiber morphology. XRD results show the crystalline properties of polyaniline nanofiber, and FTIR results confirmed the formation of polyaniline in different monomer/oxidant molar ratios [73].

In **(2013), Sharma et al.** fabricated ultrasonicated polyaniline (PAni) and tin oxide (SnO_2) composite nanofibers using electro spinning technique for hydrogen gas sensing application. The morphology of non-woven nanofibres with highly porous and agglomerated structure of diameter around 300-500 nm was confirmed by SEM image. FTIR and UV-Vis

spectra revealed the possible incorporation of SnO_2 in PAni and confirmed the uniform attachment of PAni on the surface of SnO_2 nanostructures. XRD pattern showed the presence of tetragonal SnO_2 and the crystalline structure of SnO_2 was not affected with the incorporation of PAni. The as-prepared nanofibers of PAni/SnO_2 nanocomposite showed improved hydrogen sensing properties at very low temperature as compared to that of pristine SnO_2 nanofibers [74].

In **(2013), Jundale et al.** prepared polyaniline (PAni) nanofibers reinforced with copper oxide (CuO) nanoparticles (NPs). The films were deposited on glass substrates by using spin coating technique. Polyaniline (PAni) have been synthesized by chemical oxidative polymerization method with monomer aniline in presence of $(NH_4)_2S_2O_8$ as an oxidant at 0 ^oC. The copper oxide (CuO) nanoparticles were synthesized by sol–gel method. Structural analysis showed that the crystal structure of CuO is not disturbed in the PAni–CuO hybrid nanocomposite. Surface morphology study shows the uniform distribution of CuO nanoparticles in PAni matrix. FTIR and UV–Vis studies confirm the presence of polyaniline in emeraldine base form in the composites and suggest incorporation of CuO in polymer. Two probe electrical resistivity measurements of nanocomposites (NCs) film revealed that the resistivity of PAni increases with increasing content of CuO NPs [75].

In **(2013), Babu1 et al.** synthesized conductive polyaniline by doping with inorganic and organic acids, namely Hydrochloric acid (HCl) and ±10-camphor sulfonic acid (CSA). The direct current (DC) conductivities (σ_{DC}) were found to be about 9.5×10^{-8}, 1.8, and 95.8 S/cm for PAni base, PAni (HCl) and PAni (CSA), respectively. σ_{DC} was measured down to a temperature of ~100 K and the apparent change in the activation energies were found to be 98.16, 74.40, and 57.24 meV for PAni base, PAni

(HCl) and PAni (CSA) respectively. σ_{DC} was less temperature dependent near room temperature, further decrease in temperature the σ_{DC} was strongly dependent. Photoluminescence (PL) peaks at 322.5, 581.4 and 644.2 nm were observed. [76].

In **(2014), Bari et al.** prepared nanocrystalline SnO_2 thin films using sol-gel dip coating technique. The starting precursor was used as tin chloride dihydrate ($SnCl_2.2H_2O$), ethanol and glycerin. The prepared thin films showed good selectivity to H_2 gas against LPG, CO_2, CO, NH_3, C_2H_5OH, Cl_2 and H_2S gases. It was found that the nanocrystalline SnO_2 thin films gives maximum H_2 gas response (S= 360) at 75 ^oC. The H_2 sensor showed fast speed of response ($T_{Response}$=2s) and quick recover ($T_{Recover}$= 8 s). The conductivity of each sample was observed to be increasing with an increase in temperature range between 50 ^oC and 150 ^oC in steps of 25 ^oC [77].

In **(2014), Ate et al.** synthesized CuO nanowires by thermal oxidation method. Ultrafast with high-performance CuO nanowires UV/IR photodetectors was fabricated using CuO nanowires photodetector with platinum (Pt) contact electrodes and its optoelectronic properties were examined. The results of the UV/IR photodetector exhibited a high sensitivity to UV 390 nm, Blue 410 nm ultraviolet light and 850 nm, 940 nm infrared light. The response and recovery time were also fast [78].

In **(2015), Zhu et al.** synthesized three new polyaniline (PAni) micro/nanostructures featuring square nanosheets, microspheres and micro disks via hydrothermal method. Uniform sizes and thickness of highly crystalline PAni square structural nanosheets could be tuned by the oxidative polymerization in the presence of cetyltrimethylammonium bromide (CTAB) as a template. Mechanistic studies indicate that concentrations of aniline and CTAB, reaction temperature and time had

great influence on the morphology of PAni polymers. Particularly, CTAB was essential to determine the morphology of synthetic PAni. In aqueous solution at extremely high temperature and pressure, CTAB provided various self-assembly of micelles, such as spherical micelle, planar bilayer, and lamellar phase, in which corresponding micro/nanostructures were formed. This hydrothermal fabrication gave an excellent example for the preparation of well-defined two-dimensional PAni micro/nanomaterials and potentially for other synthetic polymers [79].

In **(2015), Thenmozhi et al.** synthesized SnO_2 nanoparticles by microwave assisted solution method using $SnCl_2 \cdot 2H_2O$ as a precursor. Polyaniline doped tin oxide (PAni/ SnO_2) nanoparticles were prepared by an in situe polymerization of aniline in the presence of as-synthesized SnO_2 nanoparticles. The X-ray analysis showed that the obtained nanoparticles were SnO_2 and its crystallite size was in the range of 10-21 nm and for PAni doped SnO_2 nanoparticles, SEM micrographs indicated the presence of tin oxide nanoparticles in the PAni matrix [80].

In **(2015), Sharma et al.** synthesized and characterized polyaniline and aluminum doped tin oxide (SnO_2:Al/PAni) nanofibers for hydrogen gas sensing application. SnO_2:Al/PAni composite nanofibers had been fabricated via electrospinning technique and subsequent calcination procedure. SEM revealed the nanofibers with the diameter around 200-300 nm formed a non-woven material with highly porous and agglomerated structure. FTIR and UV-Vis spectra revealed the possible incorporation of SnO_2:Al in PAni and confirmed the uniform attachment of PAni on the surface of SnO_2:Al nanostructures. XRD showed peak broadening and the peak positions shift from standard values, indicating presence of aluminum doped tin oxide in nanoparticles form in the polyaniline (PAni) matrix. On exposure to hydrogen gas (1000 ppm), it was found that the nanofibers of

SnO_2:Al/PAni composite showed high sensitivity at 48 ^oC with relatively faster response/recovery as compared to pure SnO_2 and Al doped SnO_2 nanofibers [81].

In **(2015), Tomar et al.** prepared polyaniline (PAni) doped SnO_2 thin films sensors by chemical route and studied their properties towards the trace level detection of NO_2 gas. A good correlation had been identified between the microstructural and gas sensing properties of these prepared sensors. Out of those films, 1% PAni doped SnO_2 sensor showed high sensitivity towards NO_2 gas along with a sensitivity of 3.01×10^2 at 40 ^oC for 10 ppm of gas. On exposure to NO_2 gas, resistance of all sensors increased to a large extent, even greater than three orders of magnitude. These changes in resistance upon removal of NO_2 gas were found to be reversible in nature and the prepared composite film sensors showed good sensitivity with relatively faster response/recovery speeds [82].

In **(2014), Murugan et al.** prepared polyaniline-SnO_2 (PAni-SnO_2) hybrid materials with varied SnO_2 content by chemical oxidative polymerization method. The prepared materials were characterized by FTIR, XRD and SEM analyses. Sensitivity of the materials towards toluene was measured at room temperature from their conductivity change. The PAni-SnO_2 composite with 40 wt. % SnO_2 exhibited highest sensitivity. In situ synthesis enhanced the sensitivity of the materials over their physical mixture. This might be due to the formation of higher number of p-n heterojunctions during in situe synthesis [83].

In **(2015), Ashokan et al.** polyaniline was synthesized by chemical oxidized method and preparation of CuO nanoparticles using ethanol solvents by sol-gel route. The prepared composite samples are equal ratio of PANI/CuO (1:1) were dissolved in m-cresol solvent and were coated on glass substrate by nebulizer spray pyrolysis technique at different

temperature (100˚C, 150˚C and 200˚C). XRD study confirms the crystalline nature of CuO peaks and shows the CuO interaction with PAni structure. The SEM study shows glouber and granular particles on the surface of PAni/CuO films. FTIR spectrum reveals that the intensity of peak is increased with the increasing temperature of the sample [84].

In **(2015), Nadaf and Venkatesh.** synthesized PAni-CuO nanocomposites by oxidative polymerization. The XRD pattern shows that the crystallization process changes with different weight percentage CuO. The degree of crystallinity increased in PAni-CuO nanocomposites with increase in weight percentage of CuO nanoparticles and clearly indicated the homogeneous distributions of nanoparticles in the polymer matrix. Morphology analysis of all the samples was done with help of SEM images [85].

In **(2016), Bhagwat et al.** synthesized (PAni) nanofibers by a facile rapid oxidative polymerization of aniline hydrochloride and ammonium persulfate at high temperature (60 ^{o}C). The XRD analysis ascertained the formation of PAni with nanocrystalline nature which showed three sharp peaks at 2 θ = 15.14^{o}, 19.36^{o}, 24.48^{o}, which corresponds to (011), (020) and (200) crystal planes of PAni, and average crystallite size 30 nm. FTIR pattern confirmed the formation of PAni. SEM analysis had revealed homogeneous fibrous morphology of PAni nanofibers, a well formed mesh of interconnected and entangled PAni nanofibers over the scanned area. The UV-Vis spectroscopic analysis showed three major absorption peaks at 256.73, 361.17 and 480.95 nm which confirmed the PAni formation with conducting state [86].

In **(2016), Talegaonkar and Patil.** prepared nanocomposites of PAni-SnO_2 with three different molar concentrations of SnO_2 using in situe oxidative polymerization of aniline in presence of SnO_2. UV-Visible

spectroscopy of prepared samples of PAni-SnO_2 revealed emraldine salt phase of polyaniline. XRD patterns reflect the nano crystallite size of PAni-SnO_2 composite. Transmission electron microscopic study confirms the nano-sized of prepared composite samples. Scanning Electron Microscopy of nanocomposite showed change in surface morphology with the variation in concentration of SnO_2. PAni-SnO_2 (0.25 M) nanocomposite exhibit a response to CO_2 at quit higher temperature. The effects of surface microstructure with variation in SnO_2 concentrations and surface activation with CuO on the sensor response, selectivity, recovery and long term durability of the sensor in the presence of NH_3 and other gases were studied and discussed. SnO_2 loaded PAni was outstanding in promoting the NH_3 gas sensing performance of the material. CuO as an activator in PAni-SnO_2 enhanced ammonia sensing performance of the prepared sensor samples at room temperature [87].

In **(2016**) **Nadaf et al.** synthesized Tin Oxide (SnO_2) nanoparticles by co-precipitation method. Aniline was polymerized in the suspension of SnO_2. Ammonium per sulphate was used as oxidizing reagent to form organic-inorganic nanocomposite materials. By this way SnO_2 nanoparticles were embedded in PAni matrix. SEM images revealed that the as-synthesized powders contained spherical particles and SnO_2 was uniformly mixed within PAni matrix. As-synthesized PAni – SnO_2 nanocomposites had been tested for gas sensing applications [88]**.**

In **(2016), Talwar.** synthesized PAni-SnO_2 nanocomposites through chemical polymerization method. PAni-SnO_2 nanocomposites were explored for ammonia gas sensing at room temperature. These composites exhibited excellent sensor response for ammonia gas, where optimum sensor response was observed with the PAni-SnO_2 composite having 20 wt. % SnO_2 [89].

In **(2017), Sathiya et al.** synthesize copper oxide nanoparticles from various concentrations of $CuCl_2.2H_2O$ (0.1 M - 0.5 M) precursors by using microwave assisted co-precipitation method. Both CuO and Cu_2O phases were observed from X-ray diffraction (XRD). The particle size of 43 to 27 nm determined from XRD data using Scherrer's formula was in good relation . The existence of reasonably uniform size and shape was clear from SEM. The band gap was determined from the UV-Vis absorption peaks. These results were also related to electrical conductivity at low temperatures which illustrate different types of conduction mechanisms. The samples showed semiconducting behavior with improved electrical conductivity. Finally, the material was proposed to have applications in designing gas sensors and also in regulating electrical conductivity in drug delivery systems [90].

In **(2017), Souzaa et al.** prepared a hybrid nanocomposite based on a polymer matrix constituted of Polyaniline Emeraldine-salt form (PAni-ES) reinforced by copper oxide II (CuO) particles by polymerization method. XRD technique allowed the visualization of the polymer amorphization in the nanocomposite form, suggesting an interaction between both phases. The FTIR spectra confirmed this molecular interaction due to the blue shift of the characteristic absorption peaks of PANI-ES in the nanocomposite form. SEM images revealed that the polymer nanofiber morphology was no longer observed in the nanocomposite. The CuO spherical particles are randomly dispersed in the polymer matrix. The electrical conductivity showed an increase of 60% in the nanocomposite material [91].

In **(2018), Esmaeeli et al.** copper oxide- polyaniline nanofiber modified fluorine doped tin oxide (CuO/ PAni NFs/FTO) electrode is introduced as a non-enzymatic glucose sensor. PAni NFs were polymerized

by a chemical method and through a cellulose ester membrane. These fibers were dip coated on FTO and then CuO particles were deposited on PAni NFs by the electrode position method (CuO/ PAni NFs). The SEM image of Polyaniline clearly indicates that the polymer possesses nanofiber like structure According to the XRD pattern of PAni NFs , a broad peak at $2\theta \approx 20°$ is related to the amorphous structure of PAni and the peaks at 26, 37, 42, 51, 61 and 66° are related to (110), (111), (200), (211), (220) and (310) miller indices of CuO crystal [92].

1.13 Objectives of the study

1- Synthesis of polyaniline and metal oxides (tin oxide (SnO_2) and copper oxide (CuO)) nanostructures by using hydrothermal technique.

2- Preparation of PAni, SnO_2 and CuO thin films, and their composites with SnO_2 and CuO thin films by spin coating technique**.**

3- Study of the mixing effect on structure, optical and electrical properties of Inorganic – Polyaniline.

4- Evaluation of the use of PAni, SnO_2 and CuO, nanostructure composites of PAni/SnO_2 and PAni/CuO thin films in some optoelectronic applications such as photoconductive detector and gas sensing.